Behavioral/Systems/Cognitive

Semicircular Canal Size Determines the Developmental Onset of Angular Vestibuloocular Reflexes in Larval *Xenopus*

François M. Lambert,[1,2]* James C. Beck,[2,3]* Robert Baker,[2] and Hans Straka[1]

[1]Laboratoire de Neurobiologie des Réseaux Sensorimoteurs, Centre National de la Recherche Scientifique, Unité Mixte de Recherche 7060, Université Paris Descartes, 75270 Paris Cedex 06, France, [2]Department of Physiology and Neuroscience, New York University School of Medicine, New York, New York 10016, and [3]Department of Biology, Long Island University, Brooklyn, New York 11201

Semicircular canals have been sensors of angular acceleration for 450 million years. This vertebrate adaptation enhances survival by implementing postural and visual stabilization during motion in a three-dimensional environment. We used an integrated neuroethological approach in larval *Xenopus* to demonstrate that semicircular canal dimensions, and not the function of other elements, determines the onset of angular acceleration detection. Before angular vestibuloocular function in either the vertical or horizontal planes, at stages 47 and 48, respectively, each individual component of the vestibuloocular system was shown to be operational: extraocular muscles could be activated, central neural pathways were complete, and canal hair cells were capable of evoking graded responses. For *Xenopus*, a minimum semicircular canal lumen radius of 60 μm was necessary to permit endolymph displacement sufficient for sensor function at peak accelerations of 400°/s^2. An intra-animal comparison demonstrated that this size is reached in the vertical canals earlier in development than in the horizontal canals, corresponding to the earlier onset of vertical canal-activated ocular motor behavior. Because size constitutes a biophysical threshold for canal-evoked behavior in other vertebrates, such as zebrafish, we suggest that the semicircular canal lumen and canal circuit radius are limiting the onset of vestibular function in all small vertebrates. Given that the onset of gravitoinertial acceleration detection precedes angular acceleration detection by up to 10 d in *Xenopus*, these results question how the known precise spatial patterning of utricular and canal afferents in adults is achieved during development.

Key words: **vestibular; vestibuloocular reflex; otolith; zebrafish; development; extraocular**

Introduction

Semicircular canal and otolith organs have supported vertebrate survival in three-dimensional environments in water, on land, or in air for 450 million years (Baker and Gilland, 1996). By detecting angular and linear acceleration that result from self-motion, these vestibular sensors provide the necessary signals to generate oculomotor and postural reflexes (Walls, 1962; Land, 1999; Spoor et al., 2002). The transformation of these sensory signals into spatially precise motor commands for gaze and posture stabilization, occurs by specific convergence of semicircular canal and otolith signals in central vestibular neurons (Straka and Dieringer, 2004) and is necessary to resolve the ambiguity of otolith signals related to translational linear acceleration and head tilt (Angelaki, 2004).

Given the necessity of functional vestibular end organs for sensing head/body motion during locomotion, a rapid ontogenetic onset of both semicircular canal and otolith function would be expected to assist in confronting the consequences of body motion in space. In larval teleosts (Beck et al., 2004a; Beck and Baker, 2005) as well as in *Xenopus* (Horn et al., 1986), compensatory otolith-driven eye movements activated by gravitoinertial stimuli (gVOR) appear immediately after hatching. In contrast, at least in larval teleosts, semicircular canal evoked eye movements are considerably delayed (Beck et al., 2004a). The absence of an angular vestibuloocular reflex (aVOR) is surprising, because swimming in these animals is accompanied by undulatory body movements in the horizontal plane that generate angular head accelerations that make compensatory eye movements indispensable for retinal image stabilization.

A shift in the onset of aVOR might be related to delayed development and/or maturation of the active elements of the vestibuloocular system: hair cells, central neuronal pathways, or extraocular musculature. Alternatively, passive components of the vestibuloocular system might delay aVOR onset, namely the size of the semicircular canals themselves. Canal size determines, to a considerable extent, the sensitivity of this sensory organ to detect angular head acceleration (Muller, 1999; Rabbitt et al., 2004; Hullar, 2006). However, models linking semicircular canal geometry to locomotor performance have failed to yield a general rule (Mayne, 1950; Jones and Spells, 1963; Oman et al., 1987; Muller, 1999; Rabbitt et al., 2004) (for review, see Hullar, 2006). Nonetheless, experimental data (Yang and Hullar, 2007; Lasker et al., 2008) and theoretical considerations indicate that canal sen-

Received March 26, 2008; revised June 30, 2008; accepted July 2, 2008.

This work was supported by the Centre National de la Recherche Scientifique, Centre National d'Études Spatiales (H.S., F.M.L.), and National Institutes of Health (J.C.B., R.B.). We thank Dores Chu for assistance with animal care.

*F.M.L. and J.C.B. contributed equally to this work.

Correspondence should be addressed to Dr. Hans Straka, Laboratoire de Neurobiologie des Réseaux Sensorimoteurs, Centre National de la Recherche Scientifique, Unité Mixte de Recherche 7060, Université Paris Descartes, 45 rue des Saints-Pères, 75270 Paris Cedex 06, France. E-mail: hans.straka@univ-paris5.fr.

DOI:10.1523/JNEUROSCI.1288-08.2008

 0270-6474/08/288086-10$15.00/0

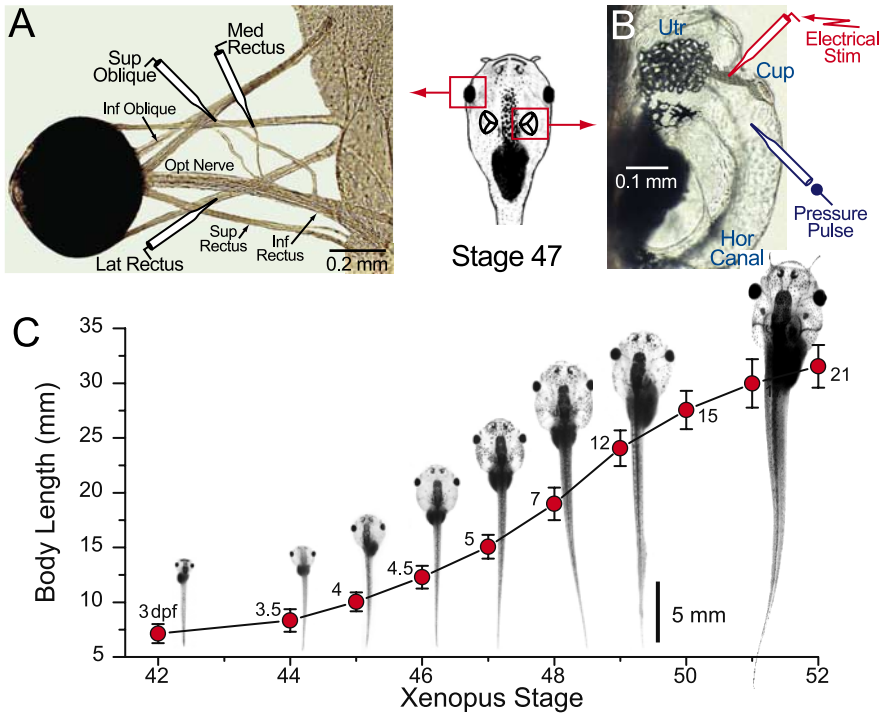

Figure 1. Schematic depicting locations of nerve recording and electrical and pressure stimulation sites in the labyrinth in larval *Xenopus*. ***A***, ***B***, The activity of motor nerves innervating extraocular muscles were recorded with suction electrodes (***A***) after either electrical stimulation (Stim) of an identified semicircular canal nerve or displacement of the canal cupula (Cup) by pressure injection of endolymph Ringer's solution, e.g., into the horizontal (Hor) canal (***B***). ***C***, Graph of body length (mean ± SD) versus developmental stage according to Nieuwkoop and Faber (1994). Superimposed on the graph is a photomontage of larval *Xenopus* from stages 42–49 showing the significant change in length and head size with age. The peak growth in larval size occurs between stages 46 and 49. Adjacent to each marker on the graph are the ages of the larvae in days postfertilization. Inf, Inferior; Lat, lateral; Med, medial; Opt, optic; Sup, superior; Utr, utricle.

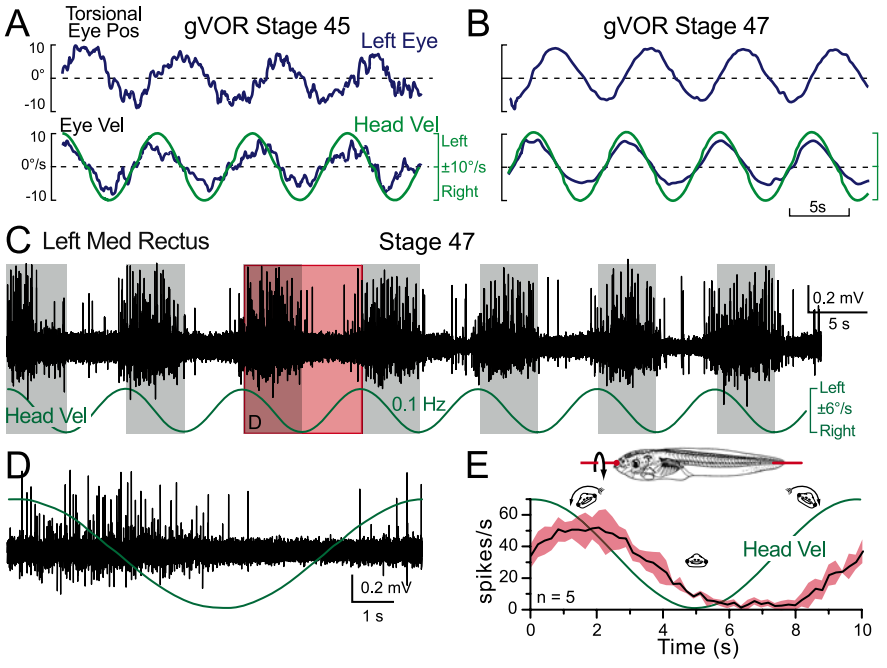

Figure 2. VOR behavior and extraocular nerve discharge of larval *Xenopus* in response to horizontal axis rotation. ***A***, ***B***, Larval *Xenopus* exhibit a robust gVOR to dynamic rotation (0.125 Hz; ±10°/s) in the horizontal (roll) plane at stage 45 (***A***) that becomes more refined by stage 47 (***B***). ***C***, ***D***, Suction electrode recording of the nerve innervating the left medial rectus in a stage 47 animal demonstrates a strong modulation in motor neuron activity during horizontal axis rotation in the roll plane. One cycle of the recording shown in ***C*** at an extended time scale is shown in ***D***. ***E***, Averaged response ± SD (red area) to horizontal axis rotation from five stage 47 larvae show discharge modulation correlated with head velocity. Pos, Position; Vel, velocity; Med, medial.

sitivity increases with both a larger canal lumen and circuit radius (Muller, 1999; Rabbitt et al., 2004; Hullar, 2006). A corollary to this work suggests that a minimum dimension for semicircular canals must be achieved in order for angular head accelerations to elicit motor commands necessary for gaze stabilization.

Here, we used larval *Xenopus* to study the development and function of semicircular canal and otolith-evoked eye movements. The hypothesis that canal size limits the onset of oculomotor function was tested by behavioral and electrophysiological analyses *in vitro* and *in vivo*. Because all elements of the aVOR pathway, from hair cells through central neurons to extraocular muscles, were found to be functional before the onset of behavior, semicircular canal size is concluded to determine the ontogenetic onset of aVOR function.

Materials and Methods

Behavioral experiments and animals. Xenopus laevis tadpoles were obtained from an authorized supplier and kept in aquaria at 18°C. Developmental stages (42–52) were determined according to the study by Nieuwkoop and Faber (1994). For behavioral tests, tadpoles were restrained in a low melting temperature agarose (2.0%; Sigma type VII-A), affixed to a thin Sylgard disk, and placed within a glass holder (Beck et al., 2004a,b). This left eyes and mouth free, permitting unrestricted eye movements and normal respiration.

Utricular vestibular stimulation. Vertical and torsional eye movements were elicited with a servocontrolled turntable that provided dynamic changes of the head with respect to gravity in the pitch or roll plane (Beck and Baker, 2005). Sinusoidal stimuli had discrete frequencies of 0.032–1.0 Hz and velocity amplitudes of ±10–60°/s.

Horizontal optokinetic and angular vestibular stimulation. Horizontal eye movements were evoked with a servocontrolled motorized vertical-axis turn-table providing angular vestibular acceleration as described previously (Beck et al., 2004a,b). Optokinetic stimulation was elicited with sinusoidal rotations of a black and white striped drum. Vestibular stimulation was generated with sinusoidal rotations of discrete frequencies between 0.065 and 1.0 Hz and maximal velocity amplitudes of ±10–60°/s. Accordingly, a stimulus of ±60°/s at 1 Hz produced head peak accelerations of ~400°/s^2. During vestibular stimulation, the eye position was recorded noninvasively in the dark by using infrared video images of the eye that were processed in real time (60 Hz) using custom video processing algorithms written in LabView (Beck et al., 2004b). Determination of gain (eye velocity/stimulus velocity) and phase relation (difference between head and eye velocity peaks) was performed in Matlab.

Subsequent to all behavioral experiments, larvae were anesthetized with 3-aminobenzoic

acid ethyl ester (MS-222; 0.03%) in a Ringer's solution [containing (in mM) 75 NaCl, 25 $NaHCO_3$, 2 $CaCl_2$, 2 KCl, 0.5 $MgCl_2$, and 11 glucose, pH 7.4] and the otic vesicles exposed to visualize individual semicircular canals for digital photomicroscopy. Measurements of the semicircular canal lumen and of the horizontal canal circuit radius were made with SigmaScan Pro and ImageJ software. Statistical tests were made using the Mann–Whitney *U* test (unpaired parameters) and the Wilcoxon signed-rank nonparametric test (paired parameters; Prism; Graphpad Software).

Electrophysiological experiments. The discharge of extraocular motor nerves innervating the medial and lateral recti and superior oblique extraocular muscles were recorded in larval *Xenopus* that were decerebrated previously under deep anesthesia with 0.1% MS-222. After transection of the optic nerves, animals were affixed to a Sylgard chamber (volume, 2.4 ml) that was continuously perfused with oxygenated Ringer's solution (16 ± 0.1°C) at a rate of 1.3–2.1 ml/min. The chamber was mounted on a computer-controlled, motorized two-axis turn-table with the animals centered in the horizontal and vertical rotation axes to provide natural activation of semicircular canals and otolith organs. Sinusoidal rotations (0.1–1.0 Hz) were performed with amplitudes of ±6–60°/s. Selective stimulation of a single vertical semicircular canal pair was achieved by orienting animals sideways in the recording chamber with the head pointing 45° upward such that one anterior–posterior vertical semicircular canal plane was oriented in the horizontal plane in the center of the vertical rotation axis. This position specifically stimulated one vertical semicircular canal pair without changing the position of the utricle with respect to the gravity vector. For recordings of extraocular motor nerve discharge, identified motor nerve branches were recorded (EXT 10–2F; NPI Electronics) with individually adjusted suction glass electrodes after being disconnected from their target muscle (see Fig. 1*A*).

Mechanically evoked displacements of the semicircular canal cupula in the on direction were achieved by inserting a beveled microelectrode (tip diameter, 5–8 μm, 30°) filled with artificial endolymph Ringer's solution (Eatock et al., 1987) into the canal and delivering short pressure pulses (1 s, 1 bar) (see Fig. 1*B*). For electrical stimulation of the horizontal semicircular canal nerve, the otic capsule was opened and the semicircular canal ampulla removed. The innervating nerve branch was isolated and stimulated with short current pulses (0.2 ms; 1–5 μA) across individually adjusted suction electrodes (Straka et al., 2003) (see Fig. 1*B*). In all electrophysiological experiments, responses were digitized, stored on computer and analyzed off-line (CED 1401, Signal, Spike 2; Cambridge Electronic Design).

Resting discharge rates of extraocular motor nerves and their modulation during sinusoidal rotation or pressure pulse injection of endolymph Ringer's solution into semicircular canals were calculated from multiunit recordings. Discharge rates were determined by setting an amplitude threshold that included all spikes for the analysis with a minimum interval of 2 ms between individual spikes. Underestimating the discharge rate because of superimposition of multiple spikes at high firing rates was unlikely because the spike widths were ~1.5 ms, the maximal peak discharge rate was ~100 Hz, and the rates were averaged over 30 cycles. Because multiunit activity was used for the analysis, the actual discharge depended on the number of units that were recorded in a nerve. However, the discharge rates both at rest and during stimulation were very similar among different animals at a common developmental stage as indicated by the small SD in mean discharge rates (see Figs. 2*E*, 3*E*,*H*, 7*C*,*F*).

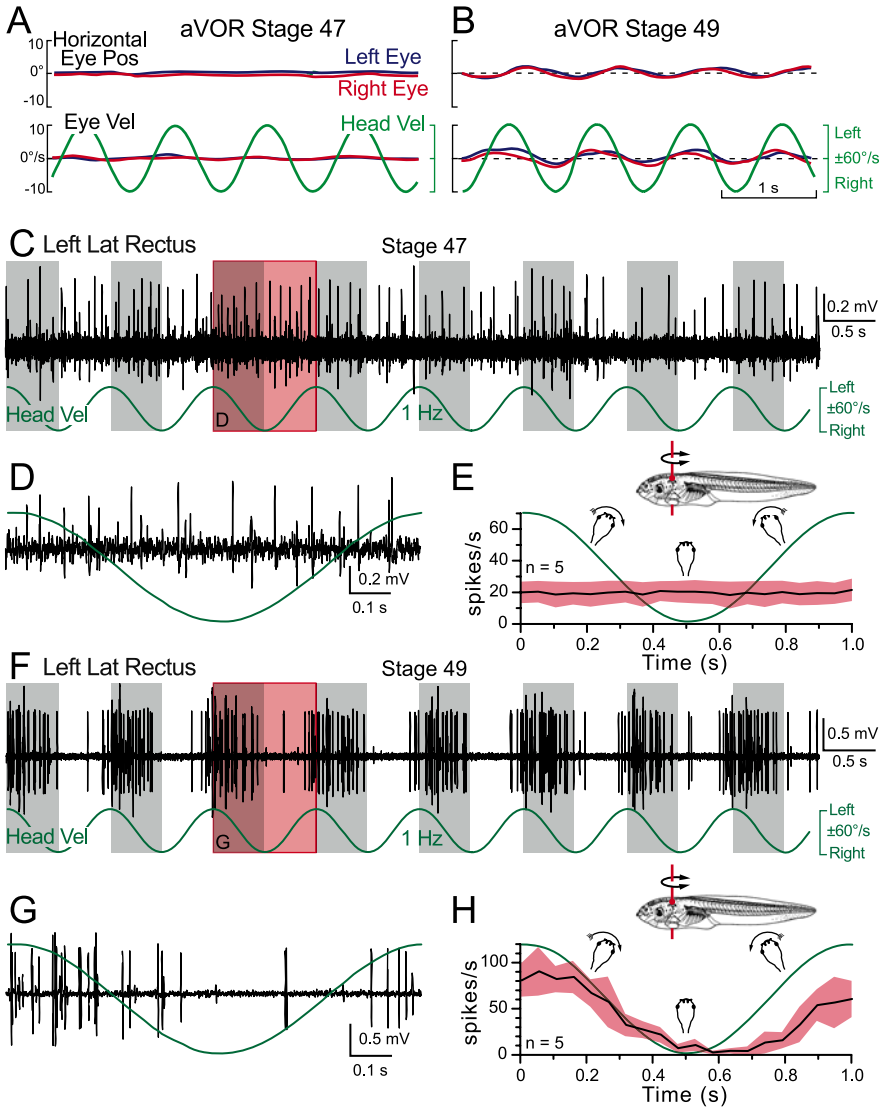

Figure 3. VOR behavior and extraocular nerve discharge of larval *Xenopus* in response to vertical axis rotation. ***A***, A stage 47 larvae did not exhibit any behavioral response during angular acceleration stimulation in the vertical axis (1 Hz; ±400°/s^2). ***B***, Only by stage 49 did *Xenopus* larvae demonstrate a reliable aVOR during angular acceleration stimulation. ***C–H***, Compatible with the behavior, the activity of the abducens nerve innervating the left lateral rectus in a stage 49 (***F–H***) but not in a stage 47 (***C–E***) *Xenopus* was modulated in response to the same stimuli. ***D***, ***G***, One cycle of the recordings in ***C*** and ***F***, respectively, at an extended time scale; the average ± SD (red area) of five animals over 30 cycles is summarized in ***E*** and ***H***, respectively. Pos, Position; Vel, velocity; Lat, lateral.

Results

Differential behavioral onset of the semicircular canal and otolith-evoked VOR

Larval frogs are freely swimming animals that need to rapidly develop appropriate vestibular reflexes for postural stabilization and gaze control during active feeding and predator avoidance soon after hatching. Within 1 d postfertilization (dpf), *Xenopus* larvae hatch (stage 24–28) (Nieuwkoop and Faber, 1994) and exhibit almost a fourfold increase in body length by 12 dpf (stage 49) (Fig. 1*C*). Vestibular sensory structures within the otic cap-

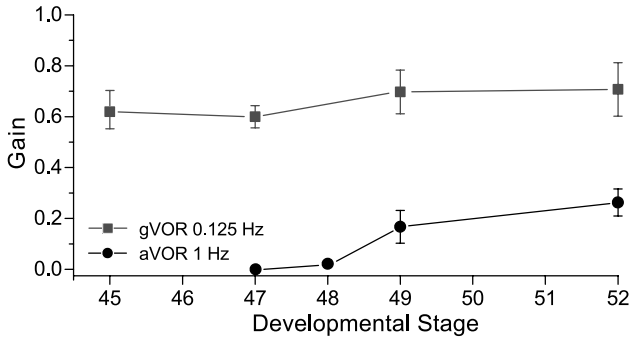

Figure 4. Ontogenetic progression of gravitoinertial and angular VOR in larval *Xenopus*. From very early stages, the utricular system of larval *Xenopus* responds well to stimulation with gVOR eye velocity gains consistently >0.6. In contrast, angular acceleration of ±400°/s^2 is unable to reliably trigger an aVOR in larval *Xenopus* until stage 49, 9 d after free swimming has commenced. Error bars indicate SD.

sule form rapidly with the otolith organs and semicircular canals completing their development by stages 42 (3 dpf) and 46–47 (4.5–5 dpf), respectively (Haddon and Lewis, 1991; Bever et al., 2003; Quick and Serrano, 2005). Swimming begins at 3 dpf (stage 42), at which time stimulation of the utricular otoliths with simple passive static position changes in the roll axis produced a counter-rotation of the eyes (data not shown) (Horn et al., 1986).

Low-frequency dynamic stimulation (0.125 Hz, ±10°/s) (supplemental Movie 1, available at www.jneurosci.org as supplemental material) of larval *Xenopus* was able to evoke robust compensatory gVOR in the dark (gain, 0.7 at stage 45) (Fig. 2*A*). Horizontal axis rotation (roll; 0.1 Hz; ±6°/s) caused a robust modulation of the resting activity (mean, 23.1 ± 6.2 spikes/s; n = 5) in the medial recti motor nerves at stage 47 with a phase-lag relative to head velocity of 68 ± 9° (Fig. 2*C–E*), compatible with the presence of otolith-evoked compensatory eye movements at this developmental stage (Figs. 2*B*, 4). The multiunit discharge exhibited symmetrical amplitude modulation with respect to the resting activity. Amplitude doubled (mean, 50.2 ± 9.2 spikes/s) during table rotation in one direction and decreased to almost zero (mean, 1.2 ± 1.1 spikes/s) during table rotation in the opposite direction (Fig. 2*C–E*). The presence of low-frequency ocular reflexes demonstrated that the peripheral and central neuronal components necessary for otolith-driven eye movements were functional shortly after hatching, at stage 42, when the animals begin self motion.

In contrast to gVOR, horizontal aVOR eye movements evoked by sinusoidal rotation around the vertical axis at 1 Hz (±60°/s, in the dark) were not present in stage 47 animals (5 dpf) (Fig. 3*A*) and could not be detected until stage 48 (7 dpf), where eye movements were just at threshold (supplemental Movies 2, 3, available at www.jneurosci.org as supplemental material). Likewise, modulation of spontaneous discharge was absent in the multiunit recordings of the lateral rectus nerve at stage 47 (Fig. 3*C–E*) and just detectable (data not shown) at stage 48 during vertical axis sinusoidal rotation (1 Hz; ±60°/s). Thus, head accelerations as large as 400°/s^2 were not able to evoke compensatory eye movements during passive body rotation at this developmental stage. It was not until stage 49 (12 dpf) that both aVOR behavior and lateral rectus motor nerve discharge was reliably modulated during vertical axis rotation (1 Hz; ±60°/s). Despite a consistent behavioral response at stage 49, eye velocity gain was relatively low (0.17 ± 0.06) (Figs. 3*B*, 4). Nevertheless, a robust modulation in amplitude was observed in the multiunit discharge from the lateral rectus. During a vertical axis table rotation at 1 Hz (±60°/s) (Fig. 3*F–H*), neural activity increased almost 2.5-fold from an average resting rate of 37.8 spikes/s (±8.6; n = 5) to 90.6 spikes/s (±22.1) with a phase lag of 43 ± 7° relative to head velocity for contraversive table rotation that almost ceased (mean, 2.6 ± 1.9 spikes/s) during ipsiversive table rotation. By stage 52 (21 dpf), there was a modest improvement in horizontal angular VOR behavior (gain, 0.26 ± 0.05) (Fig. 4).

Horizontal aVOR first begins to function a full 9 d after the onset of swimming and otolith-evoked eye movements (both at 3 dpf). The differential onset of semicircular canal (aVOR) and otolith-evoked (gVOR) behaviors might either be attributable to a delay in the maturation and functional onset of individual neuronal components of aVOR circuitry or constraint by the physical dimensions of the peripheral sensory apparatus. To test these possibilities, a combination of behavioral and electrophysiological experiments in *Xenopus* larval stages before aVOR onset was used to assess the operational state of each component of aVOR circuitry.

Vestibuloocular circuitry is functional before aVOR behavioral onset

First, a clear indication that the extraocular muscles controlling horizontal eye movements were functional, independent of the vestibular pathway, was shown with an optokinetic drum. The drum, moving sinusoidally, evoked horizontally directed eye movements from animals at stage 42 with eye velocity gain increasing with age, peaking at a gain of 0.5 (supplemental Movie 4, available at www.jneurosci.org as supplemental material). This robust optokinetic response combined with otolith-evoked eye movements demonstrated that motor plant performance and, in particular, that of the medial and lateral rectus muscles were not responsible for the delayed aVOR onset.

Before behavioral onset of aVOR at stage 48, the activity of nerves innervating the lateral and medial recti, the paired extraocular muscles responsible for conjugate horizontal eye motion, were recorded after stimulation of the horizontal canal nerve in stage 47 larval *Xenopus* (Fig. 1*A*,*B*). Electrical stimulation of the horizontal canal nerve triggered a multiunit spike discharge in the contralateral lateral rectus (Fig. 5*A*) as well as in the ipsilateral medial rectus nerve (Fig. 5*B*) with onset latencies of 9.0 ± 1.1 ms (n = 5) and 12.1 ± 1.9 ms (n = 5), respectively. The response pattern corresponded to a disynaptic connection from horizontal canal nerve afferents to lateral rectus motoneurons and a trisynaptic connection to medial rectus motoneurons (Straka and Dieringer, 1993). The difference of ~3 ms between lateral and medial rectus motoneuron discharge onset (Fig. 5, compare *A*, B) was caused by the additional synaptic delay introduced by abducens internuclear neurons (Straka and Dieringer, 1991, 1993, 2004). Activity elicited in lateral and medial recti motoneurons demonstrated that all central neuronal components required for conjugate horizontal eye motion were functional before horizontal aVOR onset.

The physiological continuity from brainstem afferents to the motor periphery before horizontal aVOR onset indicated that the sensory periphery was the likely location for the bottleneck in aVOR acquisition. Canal hair cells unable to transduce acceleration forces might prevent the expression of aVOR behavior although evidence of utricular hair cell function from behavioral and electrophysiological paradigms suggested otherwise (Fig. 2). Nevertheless, to directly test whether

impaired horizontal canal hair cell function was the reason that horizontal aVOR behavior failed to be elicited, the cupulae of this canal pair were artificially displaced in the on direction with discrete pressure pulses of endolymph Ringer's solution. A pressure pulse from an electrode inserted into the ampulla of the contralateral horizontal semicircular canal transiently increased the resting discharge (Fig. 5*C*), whereas a pulse into the ipsilateral canal transiently inhibited the nerve discharge (Fig. 5*D*). These responses are appropriate for the established push–pull organization of the horizontal aVOR neuronal circuitry (Straka and Dieringer, 2004). The modulation in lateral rectus nerve discharge was graded and could be increased by prolonging the length of the pressure stimulus (Fig. 5*E*), demonstrating that the cupula was not damaged by the stimulus paradigm.

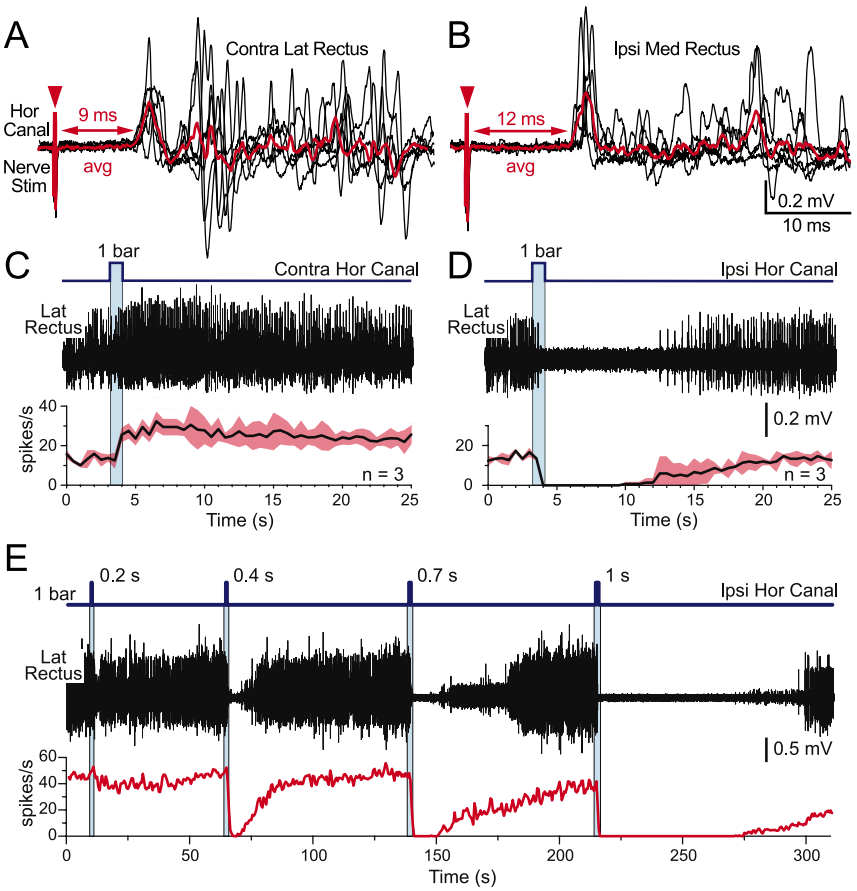

Figure 5. Electrical and pressure activation of horizontal canal afferent responses in stage 47 *Xenopus* larvae. ***A***, ***B***, Electrical stimulation of the horizontal canal nerve triggered spike activity in both the contralateral (Contra) lateral rectus (***A***) and ipsilateral (Ipsi) medial rectus nerves (***B***) as observed in six superimposed single sweep responses. Averaged responses (red) demonstrate a 3 ms difference between response onset in the two nerves. ***C***, ***D***, Lateral rectus nerve activity transiently increased (***C***) after a brief (1 s) pressure pulse into the contralateral horizontal canal and was inhibited (***D***) after a pressure pulse into the ipsilateral horizontal canal; mean ($n = 3$) ± SD (red area). ***E***, Lateral rectus nerve activity exhibited a graded inhibitory response to increasingly longer pressure pulses into the ipsilateral horizontal canal. In all cases, neural activity returned to baseline levels suggesting the cupula was not damaged by the stimulus. Other abbreviations are the same as in Figure 1. Data in ***A–D*** are from the same animal.

Angular VOR onset is likely physically constrained by canal size

As established by the electrophysiological experiments (Fig. 5), all central neuronal elements of the sensory–motor pathway, including the sensory periphery, are operational by stage 47. The implication drawn from these results is that a passive element of the horizontal canal might limit aVOR behavioral onset. For a given acceleration stimulus, the endolymph movement necessary to activate vestibular hair cells is particularly dependent on the canal lumen radius (Oman et al., 1987). Governing this endolymph movement is Poiseuille's Law, which states that the resistance to flow for a fluid through a tube is inversely proportional to the fourth power of the tube radius (Muller, 1999). As a consequence, the physical dimensions of the semicircular canals are likely parameters responsible for the delayed onset and constrained performance of the horizontal aVOR and were examined in detail.

In larval *Xenopus*, the large increase in body size between stages 45 and 49 (Fig. 1*C*) is accompanied by distinct changes in the semicircular canals. In particular, the horizontal canal increases considerably in size and the shape of the ampulla becomes more distinct between stage 45 and 49 (Fig. 6*A–D*). Quantification of the horizontal semicircular canal lumen radius at the narrowest point (Fig. 6*A–D*, arrows) and of the horizontal canal circuit radius revealed the functional onset of the horizontal aVOR to correlate with a significant increase in canal dimensions between stages 47 and 48 ($p \leq 0.01$) (Fig. 6*E*). The 1.5-fold increase in body length between stages 46 and 48 (Fig. 1*C*) was accompanied by an almost twofold increase in the canal lumen radius. The earliest above-threshold discharge modulation of the lateral rectus during yaw axis head rotation was encountered in stage 48 larvae with a canal lumen radius of 60 ± 8 μm and a circuit radius of 0.44 ± 0.06 mm ($n = 10$) (Fig. 6*E*). The relationship between canal lumen and circuit radius corresponds well with that of other vertebrates (see Fig. 9) and is predicted to be necessary to allow an undisturbed laminar endolymph flow in the semicircular canal duct system (Muller, 1999).

Different horizontal and vertical canal size correlates with differential onsets of horizontal and vertical canal aVOR

Assuming that the developmental onset of the horizontal aVOR in larval *Xenopus* is determined by the circuit and/or lumen radius of the horizontal semicircular canal then this presumed dimension threshold might also constrain the developmental onset of vertical semicircular canal-evoked aVOR behavior. To test this hypothesis, we first established when the onset of vertical aVOR occurred during ontogeny by rotating *Xenopus* larva in the plane of the vertical canals without changing the gravity vector with respect to the utricle (Fig. 7*C*, inset). In this position, vertical axis rotation of a stage 47 larva exhibited a clear modulation in the activity of the superior oblique motor nerve. The amplitude of the multiunit discharge increased almost twofold, from an average of 20.3 spikes/s (±7.4; $n = 5$) to 41.4 spikes/s (±11.0) with a phase lag of 20 ± 5° relative to head velocity (Fig. 7*A–C*), during table rotation toward the ipsilateral posterior vertical semicircular canal and decreased considerably (mean: 6.2 ± 1.9 spikes/s)

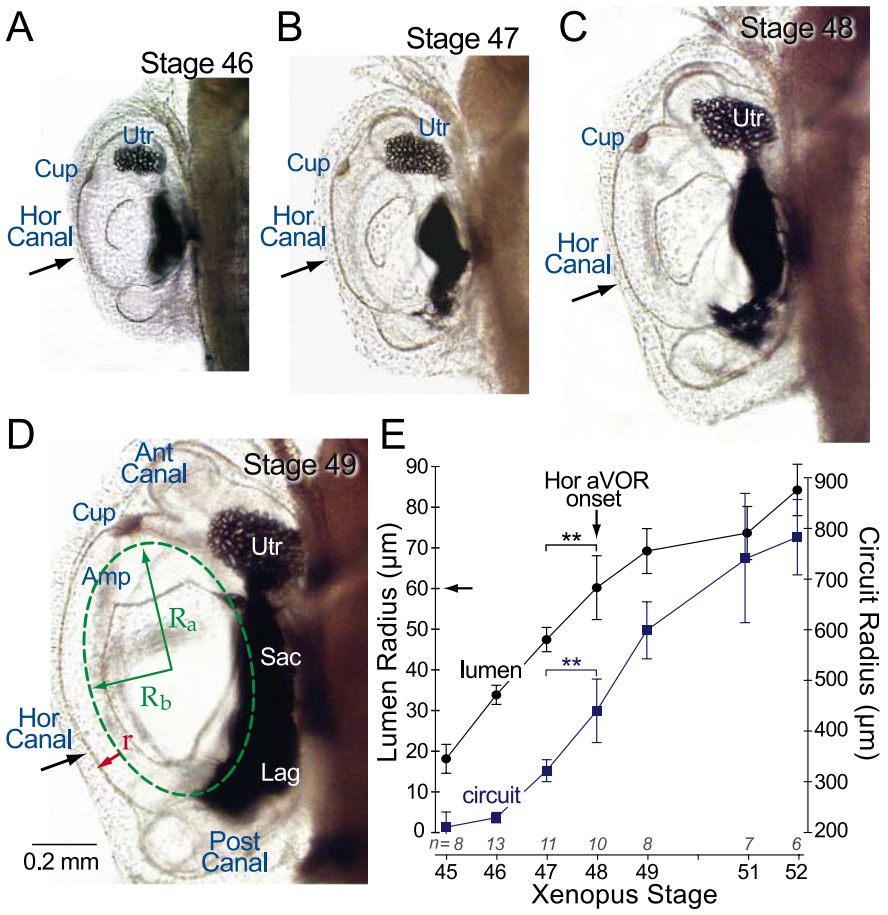

Figure 6. Semicircular canals increase in size during *Xenopus* larval development. ***A–D***, Photomicrographs of the left otic capsule, viewed dorsally from developmental stages 46–49, illustrate the increase in dimensions of the horizontal semicircular canal. Black arrows in ***A–D*** indicate the location where the canal lumen radii were measured. Superimposed in ***D*** is a schematic illustrating the parameters used to determine circuit and lumen radii. ***E***, Plot of horizontal canal lumen and circuit radius (mean ± SD) at different developmental stages before and after aVOR onset. Parameters before (stage 47) and after aVOR onset (stage 48) were significantly different (**$p \leq 0.01$, Mann–Whitney *U* test); numbers of specimens used for the analysis at each stage are indicated in ***E***. The scale bar in ***D*** applies to ***A–C***. Ant, Anterior; Amp, ampulla; Lag, lagena; R_a, R_b, large and small axes of canal circuit radius, respectively; r, radius of canal lumen; Sac, saccule. Other abbreviations are the same as in Figure 1.

during table rotation toward the contralateral anterior vertical canal. The same stimulus, however, failed to elicit a response in stage 46 larvae (Fig. 7*D–F*), establishing stage 47 as the onset of vertical aVOR. To test the function of the underlying sensory–motor network circuitry, a brief pressure pulse of endolymph Ringer's solution was applied into the ipsilateral posterior and the contralateral anterior vertical semicircular canal of stage 46 animals. The pressure stimulus was able to excite (Fig. 7*G*) and to inhibit (Fig. 7*H*), respectively, the discharge of the superior oblique nerve, appropriate for the established push–pull organization between these semicircular canals and the superior oblique nerve (Straka and Dieringer, 2004). Much like the horizontal canals, the functional connectivity from sensory to muscle periphery for the vertical canals was established before the appearance of aVOR behavior.

After determining the functional onset of the vertical aVOR, the vertical canal lumen radii were quantified in the same animals. Consistently, anatomical measurements showed that the lumen radius at the smallest point of the anterior and posterior vertical canals (Fig. 8*A*,*B*) were similar to each other but exceeded that of the horizontal canal at any given developmental stage (Fig. 8*C*). At the stage where a vertical aVOR could be elicited with a stimulation of 400°/s^2, i.e., at stage 47, the mean lumen radius of the anterior and posterior semicircular canal was 65 μm (±6; $n = 11$) (Fig. 8*C*) and, thus, very similar to that of the horizontal semicircular canal (60 μm) after onset of the horizontal aVOR behavior. This intra-animal comparison between horizontal and vertical aVOR onset supports the hypothesis that semicircular canal size limits the appearance of aVOR behavior in *Xenopus* larvae.

Canal circuit and lumen relationship

The correlation between the semicircular canal lumen radius and circuit radius in *Xenopus* larvae was assessed by visualizing the relationship between the circuit radius versus the lumen radius (Fig. 9). Superimposed on these graphs as oblique lines were the results of a model that linked canal circuit and lumen radii with canal sensitivity (Muller, 1999). The oblique sensitivity lines represent the theoretical maximum endolymph displacement in micrometers for a given angular velocity stimulus (1 radian/s or 57.3°/s). In turn, fluid displacement was determined using a homogeneous, second order equation of motion for a single, uniform duct system with constant lumen and circuit radii representing a simplified case of the semicircular canals (for additional model details, see Muller, 1999).

As larvae matured, the circuit radius remained relatively constant, whereas the lumen radius progressively increased from stages 45–47. At stage 48, where horizontal aVOR first became detectable, both circuit and lumen radii increased significantly (Fig. 6*E*), with larger changes observed in the size of the lumen radius. From stage 47–52, circuit and canal radii appeared to increase proportionately and were well fit by the regression $r = 42.2 \times r^{1.59}$ (blue line) (Fig. 9*B*), which closely paralleled the regression derived by Muller (1999): $r = 38.9 \times r^{1.60}$ (dashed line). The behavioral results observed in *Xenopus* and zebrafish (Beck et al., 2004a) combined with the presumed vestibular activity of several small adult vertebrates (Fig. 9*B*, bat, guppy, and mouse) (Muller, 1999; Calabrese and Hullar, 2006) suggests that sensitivity thresholds attributable to semicircular canal dimensions exist for all vertebrates, in particular those that develop from a very small body size.

Discussion

The ontogeny of ocular motor behavior in *Xenopus* begins with the manifestation, after hatching, of gVOR and optokinetic response (OKR) followed much later by aVOR. The delayed appearance of eye movements to horizontal angular acceleration was found not to be constrained by the physiology of either peripheral or central mechanisms but, instead, attributable to a physical factor, canal size. This interpretation was corroborated by demonstrating that vertical semicircular

canals grew larger faster and their function preceded that of the horizontal canals.

Differential onset of semicircular canal and otolith-evoked eye movements

The vestibular end organs arise from different parts of the otic placode during *Xenopus* development (Kil and Collazo, 2001). However, the formation and maturation of semicircular canal and otolith organs occur at different times (Nieuwkoop and Faber, 1994; Quick and Serrano, 2005). The utricular macula is well developed at stage 42/43 in *Xenopus* (Nieuwkoop and Faber, 1994), whereas the semicircular canals appear as paired axial protrusions and are not morphologically complete until stage 46–47 (Haddon and Lewis, 1991) at ~5 dpf (Bever et al., 2003). A similar disparate sequence for the formation of the semicircular canal and otolith organs occurs in salamanders (Wiederhold et al., 1995) and zebrafish (Haddon and Lewis, 1996; Bever and Fekete, 2002; Whitfield et al., 2002). In *Xenopus*, earlier function of the utricle with respect to the semicircular canals was suggested by counter-rotation of the eyes to static (Horn et al., 1986) and low-frequency, dynamic tilt with respect to gravity soon after hatching (Fig. 2; supplemental Movie 1, available at www.jneurosci.org as supplemental material). The early appearance of both OKR and gVOR with robust gains indicates that these behaviors, combined with signals from the spinal central pattern generator (Combes et al., 2008), are initially sufficient for larval gaze stabilization.

Although semicircular canals were morphologically complete by stages 46–47, this condition was not sufficient for angular head movement detection (supplemental Movie 2, available at www.jneurosci.org as supplemental material). Horizontal eye movements were first detected many days after the onset of OKR and gVOR, at stage 48, and then only using suprathreshold ($\geq 400°/s^2$) peak accelerations (supplemental Movie 3, available at www.jneurosci.org as supplemental material). This observation is similar to that seen in larval teleosts, which also demonstrated a significant time difference between OKR/gVOR and horizontal aVOR onset (Beck et al., 2004a). In that study, behavioral responses were also only elicited by suprathreshold stimuli ($\geq 400°/s^2$). The observation of a differential time of onset for semicircular canal and otolith-evoked eye movements in teleosts and amphibians suggests an underlying principle common to vertebrates that mature through a series of continuously growing developmental stages.

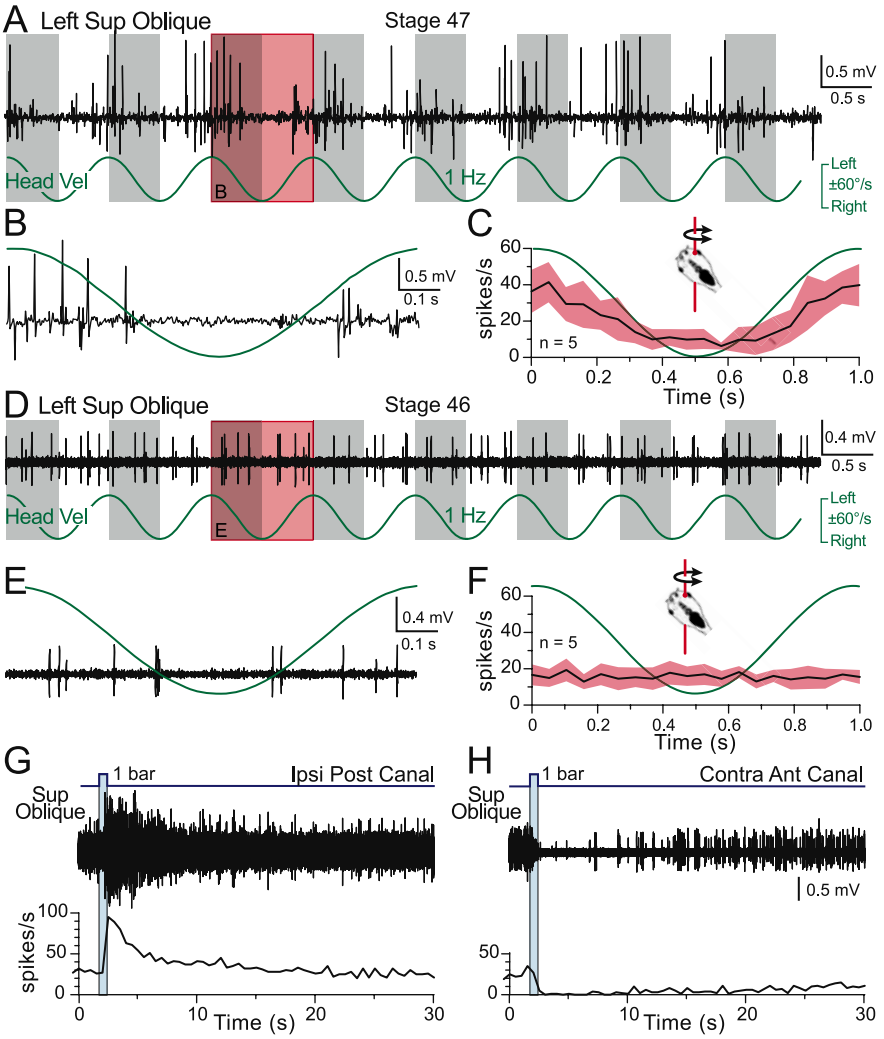

Figure 7. Extraocular nerve discharge during vertical axis rotation in larval *Xenopus*. ***A–F***, Vertical axis rotation designed to minimize utricle activation and maximally activate one vertical canal pair (***C***, inset) modulates the spike discharge of the superior (Sup) oblique nerve in stage 47 animals (***A–C***) but does not modulate nerve activity in stage 46 animals (***D–F***). ***B*** and ***E*** show one cycle of the recordings in ***A*** and ***D*** at an extended time scale, respectively; the average ± SD (red area) of five animals over 30 cycles is summarized in ***C*** and ***F***, respectively. ***G***, ***H***, A brief pressure pulse of endolymph Ringer's solution into the ipsilateral (Ipsi) posterior (Post) (***G***) and contralateral (Contra) anterior (Ant) vertical semicircular canal (***H***) in the same stage 46 specimen shown in ***D–F*** modulated the discharge of the superior oblique nerve. The scale bar in ***H*** also applies to ***G***.

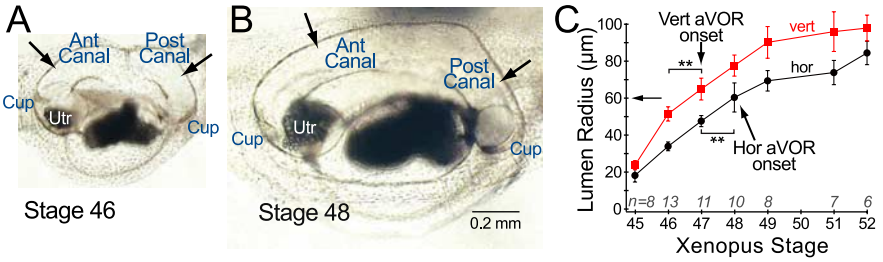

Figure 8. Photomicrographs of the left otic capsule from stage 46 and 48 *Xenopus* larvae. ***A***, ***B***, Lateral view of the anterior (Ant) and posterior (Post) vertical canals in left otic capsule. Black arrows indicate location where canal lumen radii were measured. ***C***, Plot of vertical canal lumen radius (anterior and posterior canals combined) and horizontal lumen radius (mean ± SD) at different developmental stages before and after aVOR onset. Canal lumen radii before and after horizontal aVOR onset (stage 47 and 48) and before and after vertical aVOR onset (stage 46 and 47) were significantly different (**$p \leq 0.01$; Mann–Whitney *U* test); numbers of specimens used for the analysis at each stage are indicated in ***C***. Other abbreviations are the same as in Figure 1.

Semicircular canal size as a limiting parameter for aVOR onset

Formed well before the behavioral onset of canal-evoked eye movements, the integrity of the semicircular canals of zebrafish

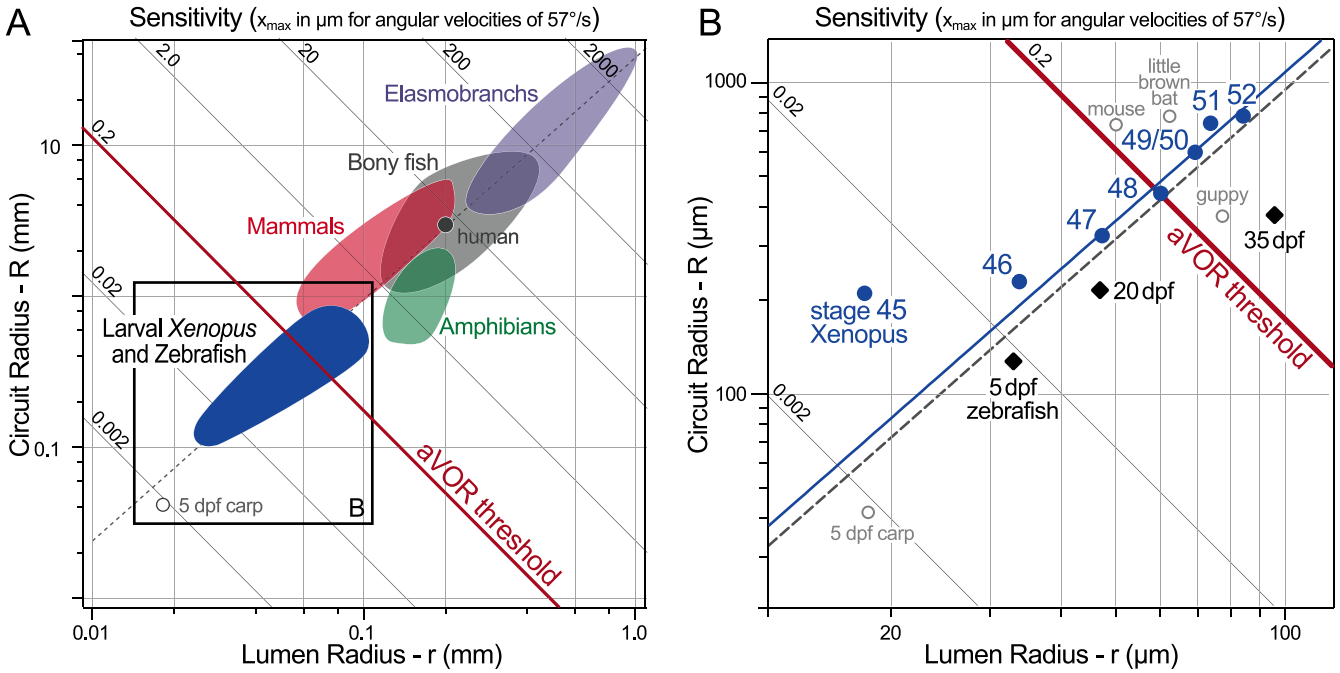

Figure 9. Plots of mean canal lumen radius (*r*) versus mean canal circuit radius (*R*) of the horizontal canals of larval *Xenopus* and zebrafish. ***A***, Superimposed are canal dimensions for selected classes of vertebrates adapted from the study by Muller (1999). Oblique lines represent theoretical endolymph displacement in micrometers for a given angular velocity (1 radian/s or 57.3°/s) and the dashed gray line is the regression line of $r = 38.9 \times r^{1.60}$ all as calculated by Muller (1999). ***B***, The solid blue line is the regression line of $r = 42.2 \times r^{1.59}$ for stage 47–52 larvae. Measurements for the horizontal canal lumen and circuit radii for larval zebrafish and mouse are from previous studies [5, 20 dpf (Bever and Fekete, 2002); 35 dpf and behavior (Beck et al., 2004b); mouse (Calabrese and Hullar, 2006)]. The mouse lumen radius is shown at its smallest estimated size. For stage 48 *Xenopus*, the horizontal aVOR rises above threshold for the first time and becomes fully active at stage 49. Based on the behavioral response of *Xenopus* and zebrafish larvae, the oblique solid red line is a generalized sensitivity threshold for vertebrate aVOR behavior for this stimulus.

and *Xenopus*, as demonstrated here, was not sufficient for triggering a physiological aVOR (Beck et al., 2004a). Nonetheless, from at least stage 47 to the onset of aVOR behavior at stage 49, both the signal transduction of cupular hair cells as well as the central neuronal pathways connecting the sensory periphery with the extraocular motor neurons was functional in *Xenopus* (Figs. 3, 5). Thus, in the absence of any apparent physiological constraint, it is likely that a physical factor may determine the behavioral onset of aVOR.

Modeling studies have implicated a number of biomechanical parameters that may play a role in the sensitivity of semicircular canals to angular acceleration. These parameters include endolymph viscosity, cupular stiffness, canal lumen, and circuit radius (for review, see Rabbitt et al., 2004). Physical laws and mathematical models argue that there must be a minimum lumen and circuit radius necessary to detect angular accelerations during naturally occurring head movements (Muller, 1999; Rabbitt, 1999). For very compact canals in small vertebrates, the dimensions of the smallest portion of the canal lumen are likely to dominate biomechanical factors affecting canal sensitivity (Rabbitt, 1999; Rabbitt et al., 2004). Indeed, as the circuit radius enlarges, the increased inertial forces that can be generated are largely offset by the increased viscous drag of the endolymph (Rabbitt, 1999). For the canal lumen, however, fluid flow resistance is inversely proportional to the fourth power of the tube radius (Muller, 1999); consequently, the 12.5 μm increase in horizontal canal lumen radius observed as larval *Xenopus* mature from stage 47 to stage 48 equates to an ~2.6-fold decrease in resistance to endolymph movement.

In addition to models of canal biomechanics, support for the hypothesis that canal size determines the onset of aVOR behavior in larval *Xenopus* comes from an intra-animal comparison. The onset of aVOR occurred by stage 48 and was correlated with a significant increase in size of the horizontal canal, as it reached an average radius of 60 μm (Fig. 6*E*). If canal radius was truly determining aVOR onset, then a similar size constraint must exist for the vertical canals. This was found to be the case. The onset of eye movements elicited by the vertical canals occurred when the canal lumen radius grew from 51 μm at stage 46 to 64 μm at stage 47 (Fig. 8*C*). The intra-animal comparison also helped militate the influence of other physiological or biomechanical factors in canal sensitivity such as endolymph and perilymph composition. These two factors were unlikely to be different between the horizontal and vertical canals because all are interconnected via the common crus. Although the structure of the cupula is likely to be similar between the canals, it is possible that the area of the cupula, and hence its stiffness (Rabbitt et al., 2004), covaries with increasing canal size. In that case, the contribution of cupular mechanics and canal radii would be indistinguishable.

Ascribing canal sensitivity to a particular canal dimension (lumen or circuit radius) has been a long-discussed and often contentious issue (Curthoys, 1982; Oman et al., 1987; Muller, 1994, 1999; Spoor et al., 2002; Hullar, 2006; Yang and Hullar, 2007). *Xenopus* (Fig. 9) have large increases in the lumen radius and smaller changes in circuit radius during development. Thus, for this species, the lumen radius is likely to be a larger factor in determining threshold. In studies of teleost oculomotor ontogeny, both larval zebrafish and medaka do not exhibit aVOR (at ~400°/s^2) until many weeks after hatching (Beck et al., 2004a). The onset of aVOR was correlated with increasing animal size and therefore increasing canal lumen size (Fig. 9). Nevertheless, as predicted by the graph shown in Figure 9 (red line), which combines our behavioral data with the canal sensitivity model of Muller (1999), a sufficiently large circuit radius may overcome limits imposed by the lumen radius.

Like *Xenopus*, mice demonstrate an age-related increase in VOR eye velocity gain (Shiga et al., 2005). Although vestibular afferent sensitivity is correlated with canal circuit radius in mouse (Yang and Hullar, 2007; Lasker et al., 2008), the sensitivity is threefold less than in larger mammals, attributed to canal lumen radius (Lasker et al., 2008). Using μCT, the horizontal semicircular canal of the C57BL/6 strain mouse was found to have a circuit radius of 725 μm and a 50–75 μm lumen radius (Calabrese and Hullar, 2006). The circuit radius of these mice matches that found in stage 50 *Xenopus* yet the range of their canal lumen radii lies near the threshold observed for aVOR onset in *Xenopus* and teleosts. Determination of the true *in vivo* dimensions of the mouse canal lumen in relation to angular acceleration sensitivity, in juveniles and adults, would help determine how significant canal lumen radii are in limiting angular acceleration sensitivity. Semicircular canal dimension is likely to be the constraining factor that determines the ontogenetic onset of aVOR not only in amphibians and teleosts but in mammals as well.

Combined semicircular canal and otolith signals for appropriate sensory–motor transformation

In mature animals, vestibular signals arising from canal and utricular afferents are transformed by second-order vestibular neurons into appropriate directional (vectorial) commands for extraocular motoneurons (Straka and Dieringer, 2004). Spatially specific canal and directionally specific otolithic signals (Rohregger and Dieringer, 2002) converge onto >50% of the second-order vestibular neurons (Straka et al., 2003). Because utricular function precedes semicircular canal function in larval *Xenopus*, how can a complex spatial pattern of afferents make appropriate connections in the absence of behavior? The spatially precise convergence could be achieved by canal afferents superimposing their rotation-specific signals onto the correct gravitational neuronal populations within the utricular scaffold. Alternatively, the canal pathways might simply rely on an exuberant production of exploratory axon collaterals and an activity-dependent Hebbian-type mechanism as in the development of the *Xenopus* retinotectal system (Witte et al., 1996). The segmental organization of the developing hindbrain also provides an independent means to guide semicircular canal and otolith afferent fibers to their appropriate connections with central vestibular targets (Fritzsch et al., 2002; Fritzsch, 2003). Many developmentally regulated genes are expressed in both transverse and longitudinally restricted domains to create a mosaic of genetically unique neuroepithelial regions that give rise to specific subsets of vestibular functional phenotypes (Glover, 2000; Straka et al., 2001; Glover, 2003). Determining which of these three possibilities is responsible for vestibular afferent mapping can be addressed with current physiological and genetic tools in *Xenopus* and zebrafish models.

References

Angelaki DE (2004) Eyes on target: what neurons must do for the vestibuloocular reflex during linear motion. J Neurophysiol 92:20–35.

Baker R, Gilland E (1996) The evolution of hindbrain visual and vestibular innovations responsible for oculomotor function. In: The acquisition of motor behavior in vertebrates (Bloedel JR, Ebner TJ, Wise SP, eds), pp 29–55. Cambridge, MA: MIT.

Beck JC, Baker R (2005) Static and dynamic measurement of otolithic VOR during the absence of canal function in larval zebrafish. Soc Neurosci Abstr 31:391.16.

Beck JC, Gilland E, Tank DW, Baker R (2004a) Quantifying the ontogeny of optokinetic and vestibuloocular behaviors in zebrafish, medaka, and goldfish. J Neurophysiol 92:3546–3561.

Beck JC, Gilland E, Baker R, Tank DW (2004b) Instrumentation for measuring oculomotor performance and plasticity in larval organisms. Methods Cell Biol 76:385–413.

Bever MM, Fekete DM (2002) Atlas of the developing inner ear in zebrafish. Dev Dyn 223:536–543.

Bever MM, Jean YY, Fekete DM (2003) Three-dimensional morphology of inner ear development in *Xenopus laevis.* Dev Dyn 227:422–430.

Calabrese DR, Hullar TE (2006) Planar relationships of the semicircular canals in two strains of mice. J Assoc Res Otolaryngol 7:151–159.

Combes D, Le Ray D, Lambert FM, Simmers J, Straka H (2008) An intrinsic feed-forward mechanism for vertebrate gaze stabilization. Curr Biol 18:R241–R243.

Curthoys IS (1982) The response of primary horizontal semicircular canal neurons in the rat and guinea pig to angular acceleration. Exp Brain Res 47:286–294.

Eatock RA, Corey DP, Hudspeth AJ (1987) Adaptation of mechanoelectrical transduction in hair cells of the bullfrog's sacculus. J Neurosci 7:2821–2836.

Fritzsch B (2003) Development of inner ear afferent connections: forming primary neurons and connecting them to the developing sensory epithelia. Brain Res Bull 60:423–433.

Fritzsch B, Beisel KW, Jones K, Fariñas I, Maklad A, Lee J, Reichardt LF (2002) Development and evolution of inner ear sensory epithelia and their innervation. J Neurobiol 53:143–156.

Glover JC (2000) Neuroepithelial "compartments" and the specification of vestibular projections. Prog Brain Res 124:3–21.

Glover JC (2003) The development of vestibulo-ocular circuitry in the chicken embryo. J Physiol (Paris) 97:17–25.

Haddon C, Lewis J (1996) Early ear development in the embryo of the zebrafish, *Danio rerio*. J Comp Neurol 365:113–128.

Haddon CM, Lewis JH (1991) Hyaluronan as a propellant for epithelial movement: the development of semicircular canals in the inner ear of *Xenopus.* Development 112:541–550.

Horn E, Lang HG, Rayer B (1986) The development of the static vestibulo-ocular reflex in the southern clawed toad, *Xenopus laevis* I. Intact animals. J Comp Physiol [A] 159:869–878.

Hullar TE (2006) Semicircular canal geometry, afferent sensitivity, and animal behavior. Anat Rec A Discov Mol Cell Evol Biol 288:466–472.

Jones GM, Spells KE (1963) A theoretical and comparative study of the functional dependence of the semicircular canal upon its physical dimensions. Proc R Soc Lond B Biol Sci 157:403–419.

Kil SH, Collazo A (2001) Origins of inner ear sensory organs revealed by fate map and time-lapse analyses. Dev Biol 233:365–379.

Land MF (1999) Motion and vision: why animals move their eyes. J Comp Physiol [A] 185:341–352.

Lasker DM, Han GC, Park HJ, Minor LB (2008) Rotational responses of vestibular–nerve afferents innervating the semicircular canals in the C57BL/6 mouse. J Assoc Res Otolaryngol, in press.

Mayne R (1950) The dynamic characteristics of the semicircular canals. J Comp Physiol Psychol 43:309–319.

Muller M (1994) Semicircular duct dimensions and sensitivity of the vertebrate vestibular system. J Theor Biol 167:239–256.

Muller M (1999) Size limitations in semicircular duct systems. J Theor Biol 198:405–437.

Nieuwkoop PD, Faber J (1994) Normal table of *Xenopus laevis* (Daudin): a systematical and chronological survey of the development from the fertilized egg till the end of metamorphosis. New York: Garland.

Oman CM, Marcus EN, Curthoys IS (1987) The influence of semicircular canal morphology on endolymph flow dynamics. An anatomically descriptive mathematical model. Acta Otolaryngol 103:1–13.

Quick QA, Serrano EE (2005) Inner ear formation during the early larval development of *Xenopus laevis.* Dev Dyn 234:791–801.

Rabbitt RD (1999) Directional coding of three-dimensional movements by the vestibular semicircular canals. Biol Cybern 80:417–431.

Rabbitt RD, Damiano ER, Grant JW (2004) Biomechanics of the vestibular semicircular canals and otolith organs. In: The vestibular system (Highstein SM, Fay RR, Popper AN, eds), pp 153–201. New York: Springer.

Rohregger M, Dieringer N (2002) Principles of linear and angular vestibuloocular reflex organization in the frog. J Neurophysiol 87:385–398.

Shiga A, Nakagawa T, Nakayama M, Endo T, Iguchi F, Kim TS, Naito Y, Ito J

(2005) Aging effects on vestibulo-ocular responses in C57BL/6 mice: comparison with alteration in auditory function. Audiol Neurootol 10:97–104.

Spoor F, Bajpai S, Hussain ST, Kumar K, Thewissen JG (2002) Vestibular evidence for the evolution of aquatic behaviour in early cetaceans. Nature 417:163–166.

Straka H, Dieringer N (1991) Internuclear neurons in the ocular motor system of frogs. J Comp Neurol 312:537–548.

Straka H, Dieringer N (1993) Electrophysiological and pharmacological characterization of vestibular inputs to identified frog abducens motoneurons and internuclear neurons in vitro. Eur J Neurosci 5:251–260.

Straka H, Dieringer N (2004) Basic organization principles of the VOR: lessons from frogs. Prog Neurobiol 73:259–309.

Straka H, Baker R, Gilland E (2001) Rhombomeric organization of vestibular pathways in larval frogs. J Comp Neurol 437:42–55.

Straka H, Holler S, Goto F, Kolb FP, Gilland E (2003) Differential spatial organization of otolith signals in frog vestibular nuclei. J Neurophysiol 90:3501–3512.

Walls GL (1962) The evolutionary history of eye movements. Vision Res 2:69–80.

Whitfield TT, Riley BB, Chiang MY, Phillips B (2002) Development of the zebrafish inner ear. Dev Dyn 223:427–458.

Wiederhold ML, Yamashita M, Larsen KA, Batten JS, Koike H, Asashima M (1995) Development of the otolith organs and semicircular canals in the Japanese red-bellied newt, *Cynops pyrrhogaster*. Hear Res 84:41–51.

Witte S, Stier H, Cline HT (1996) In vivo observations of timecourse and distribution of morphological dynamics in *Xenopus* retinotectal axon arbors. J Neurobiol 31:219–234.

Yang A, Hullar TE (2007) Relationship of semicircular canal size to vestibular-nerve afferent sensitivity in mammals. J Neurophysiol 98:3197–3205.